ELSEVIER

Electrical Power and Energy Systems 26 (2004) 423–430

ELECTRICAL POWER & ENERGY SYSTEMS

www.elsevier.com/locate/ijepes

A self-tuning power system stabilizer based on artificial neural network

Ravi Segal[a], Avdhesh Sharma[b], M.L. Kothari[c,*]

[a]GE Power Services (I) Limited, Field Engineering Services, New Delhi 110 002, India
[b]Department of Electrical Engineering, M.B.M. Engineering College, J.N.V. University, Jodhpur 342 011, India
[c]Department of Electrical Engineering, Indian Institute of Technology, Hauz Khas, New Delhi 110 016, India

Received 14 November 2001; revised 3 October 2003; accepted 7 November 2003

Abstract

This paper presents a systematic approach for designing a self-tuning power system stabilizer (PSS) based on artificial neural network (ANN). An ANN is used for self-tuning the parameters of PSS in real-time. The nodes in the input layer of the ANN receive generator terminal active power (P), reactive power (Q), and voltage (V_t), while the nodes in the output layer provide the optimum PSS parameters, e.g. stabilizing gain (K_{STAB}), time constants (T_1 and T_2). A new approach for the selection of number of neurons in the hidden layer has been proposed. Investigations reveal that the dynamic performance of the system with self-tuning PSS based on ANN (ST-ANNPSS) is quite robust over a wide range of loading conditions and equivalent reactance, X_e.

Keywords: Power system stabilizer; Artificial neural network; Small signal stability; Self-tuning controllers

1. Introduction

Power system stabilizers (PSS) have been extensively used in large power systems for enhancing stability of the system. The conventional fixed structure PSS, designed using a linear model obtained by linearizing nonlinear model around a nominal operating point provides optimum performance for the nominal operating condition and system parameters. However, the performance becomes suboptimal following deviations in system parameters and loading condition from their nominal values.

In recent years, self-tuning PSSs, variable structure PSSs, fuzzy logic PSSs and artificial neural network (ANN) based PSSs [1–5] have been proposed to provide optimum damping to the system oscillations over a wide range of system parameters and loading conditions. Two reasons are put forward for using ANN. First, since an ANN is based on parallel processing, it can provide extremely fast processing facility. The second reason for the high level of interest is the ability of ANN to realize complicated nonlinear mapping from the input space to the output space.

The ANN based PSS proposed in the literature may be classified into the following two categories.

(a) In the first category of the ANN based PSS, the ANN is used for real-time tuning of the parameters of the conventional PSS (e.g. proportional and integral gain settings of the PSS [1]). The input vector to the ANN represents the current operating condition, while the output vector comprises the optimum parameters of the conventional PSS.

The ANN-tuned PSS can be regarded as a kind of self-tuning PSSs. The main advantage of ANN-tuned PSS over a self-tuning PSSs is that the ANN-tuned PSS does not require system identification, while the conventional self-tuning PSS does.

(b) In the second category of the ANN based PSS, the ANN is designed to emulate the function of the PSS and directly computes the optimum stabilizing signal [2–5].

It may be noted that the number of training patterns required in the second category is very large, as compared to that in the first category [1,3]. Moreover, the generation of training patterns in the first category is very straightforward as compared to those in the second category.

The literature survey shows that in most of the past research work pertaining to ANN based PSS, the number of neurons in the hidden layer have been chosen arbitrarily. The main thrust of the research work presented in this paper is to address to some of the important issues pertaining to

* Corresponding author.
E-mail address: mohankothari@hotmail.com (M.L. Kothari).

0142-0615/$ - see front matter © 2004 Published by Elsevier Ltd.
doi:10.1016/j.ijepes.2003.11.010

Nomenclature

H	inertia constant
δ	angle between quadrature axis and infinite bus voltage
ω	angular speed
E_B	infinite bus voltage
T_m, T_e	mechanical and electrical torques, respectively
L_{adu}	unsaturated value of direct axis inductance
X_d	direct axis reactance
X_q	quadrature axis reactance
X'_d	direct axis transient reactance
X_l	leakage reactance
R_a	stator resistance per phase
E_{fd}	equivalent exciter voltage
E'_q	voltage proportional to d-axis flux linkages
T_R	terminal voltage transducer time constant
V_{ref}	AVR reference signal
K_A, T_A	AVR gain and time constant, respectively
v_S	stabilizing signal
T_w	washout time constant
K_{STAB}	PSS gain
T_1-T_2	PSS time constants
i_{fd}	field current
R_{fd}, L_{fd}	field winding resistance and inductance, respectively
R_e, X_e	equivalent resistance and reactance, respectively

the design and performance evaluation of ANN based PSS, e.g. selection of elements of input vector of the training patterns, number of training patterns, selection of number of neurons in the hidden layer, and performance of the system with ST-ANNPSS under wide variations in loading and line reactance X_e.

The main objectives of the research work presented in this article are:

1. To present a systematic approach for designing a multilayer feedforward artificial neural network based self-tuning PSS (ST-ANNPSS).
2. To suggest an approach for selecting the number of neurons in the hidden layer.
3. To study the dynamic performance of the system with ST-ANNPSS and hence to compare with that of conventional PSS.
4. To investigate the effect of variation of loading condition and equivalent reactance, X_e on dynamic performance of the system with ST-ANNPSS.

2. System investigated

A single machine-infinite bus (SMIB) system is considered for the present investigations. A machine connected to a large system through a transmission line may be reduced to a SMIB system, by using Thevenin's equivalent of the transmission network external to the machine. Because of the relative size of the system to which the machine is supplying power, the dynamics associated with machine will cause virtually no change in the voltage and frequency of the Thevenin's voltage E_B (infinite bus voltage). The Thevenin equivalent impedance shall henceforth be referred to as equivalent impedance (i.e. $R_e + jX_e$). The nominal parameters and the nominal operating condition of the system are given in the Appendix. IEEE type ST1A model of static excitation system has been considered. Conventional PSS comprising cascade connected lead networks with generator angular speed deviation ($\Delta\omega$) as input signal has been considered. Fig. 1 shows the small perturbation transfer function block diagram of the SMIB system relating the pertinent variables of electrical torque, speed, angle, terminal voltage, field voltage and flux linkages. This linear model has been developed, by linearizing the nonlinear differential equations around a nominal operating point [6].

3. Transfer function model of the power system stabilizer and the design considerations

Fig. 2 represents a transfer function block diagram of the system, through which an electrical torque is produced in response to speed deviation signal, $\Delta\omega$, where as GEP(s) is a transfer function of the system whose output is electrical torque and input is stabilizing signal. In order to increase damping of the rotor oscillations, a PSS utilizing shaft speed deviation as input signal must compensate for the phase-lag of GEP(s) to produce a component of the torque in phase with speed deviation [8]. The transfer function of a PSS is represented as:

$$\frac{v_S(s)}{\Delta\omega(s)} = K_{STAB}\left[\frac{(sT_w)}{(1+sT_w)}\right]\left[\frac{(1+sT_1)(1+sT_3)}{(1+sT_2)(1+sT_4)}\right]\mathrm{FILT}(s) \quad (1)$$

where K_{STAB} is stabilizer gain, FILT(s) is combined transfer function of torsional filter and input signal transducer, T_w is washout time constant and T_1, T_2, T_3, T_4 are time constants of the lead–lag networks.

An optimum stabilizer is obtained by a suitable selection of time constants T_w, T_1, T_2, T_3, T_4 and stabilizer gain K_{STAB}. Two identical lead-lag networks can be chosen for a conventional PSS (i.e. $T_1 = T_3$ and $T_2 = T_4$). This choice reduces the number of parameters to be optimized. The filter is used for attenuating the stabilizer gains at turbine-generator shaft torsional frequencies and may be neglected

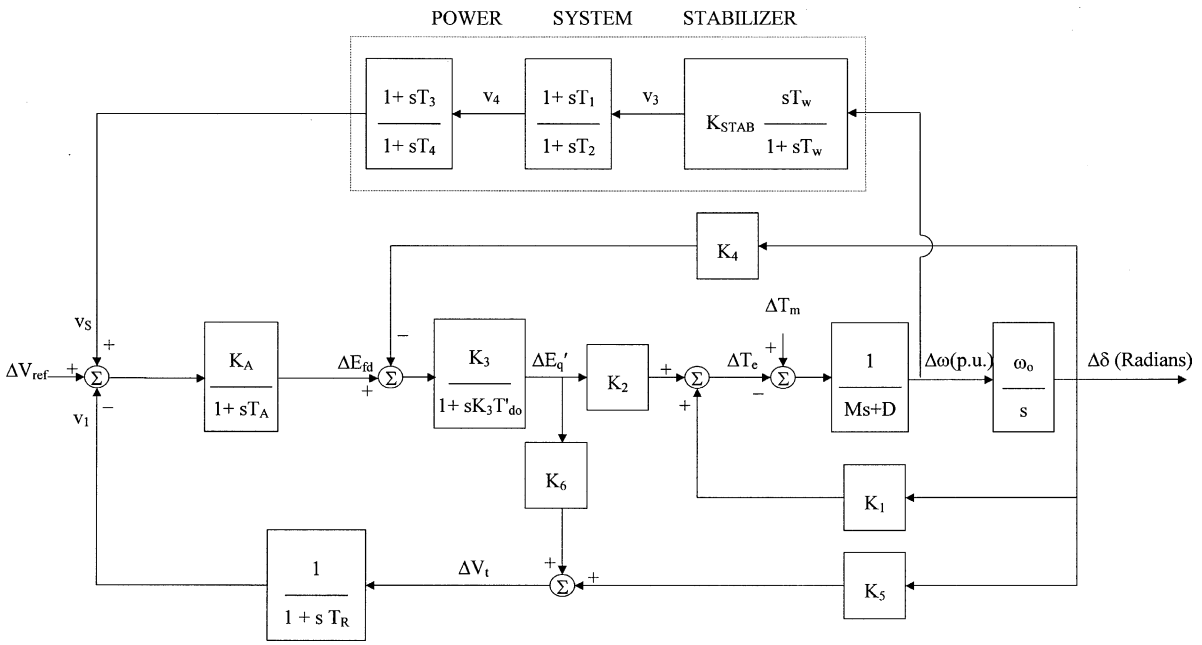

Fig. 1. Small perturbation transfer function block diagram of a single machine-infinite bus system with conventional PSS.

while designing PSS. The design considerations and the procedure for selecting the PSS parameters are as follows.

3.1. Phase lead compensation

To damp rotor oscillations, the PSS must produce a component of electrical torque in phase with the rotor speed deviation. This requires phase-lead circuits to compensate the phase-lag between exciter input (i.e. PSS output) and the resulting electrical torque. The phase characteristic of the system (i.e. GEP(s)) depends on the system parameters and the operating condition. The required phase-lead for a given operating condition and system parameters can be achieved by selecting the appropriate value of time constants T_1-T_4.

3.2. Stabilizing signal washout

The signal washout is a high-pass filter that prevents steady changes in the speed from modifying the field voltage. The value of the washout time constant T_w should be high enough to allow signals associated with oscillations in rotor speed to pass unchanged. From the viewpoint of the washout function, the value of T_w is not critical and may be in the range of 1–20 s. For local mode oscillations in the range of 0.8–2.0 Hz, a washout time constant of about 1.5 s is satisfactory. From the viewpoint of low-frequency interarea oscillations, a washout time constant of 10 s or higher is desirable.

3.3. Stabilizer gain

Ideally, the stabilizer gain should be set at a value corresponding to optimum damping. However, this is often limited by other considerations. It is set to a value, which results in satisfactory damping of the critical modes without compromising the stability of the other modes, and which does not cause excessive amplification of stabilizer input signal noise.

4. Case study

Fig. 3 depicts the schematic diagram of a synchronous generator with ST-ANNPSS. The ANN is used for tuning the parameters of the PSS in real-time. For a SMIB system, the generator terminal complex power ($P+jQ$), generator terminal voltage (V_t), equivalent reactance X_e and infinite

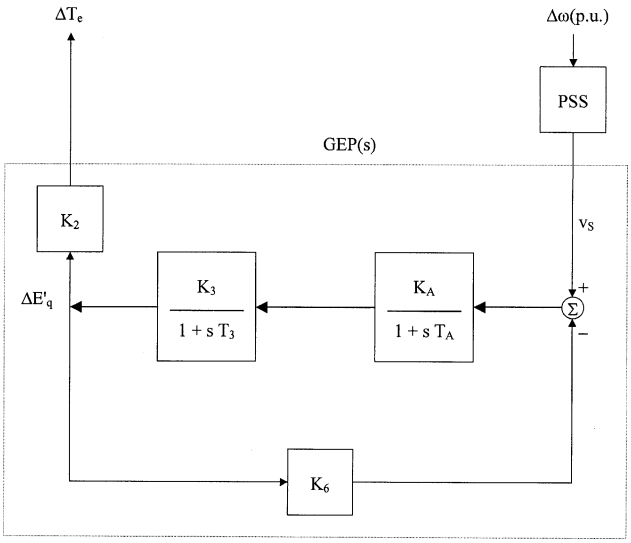

Fig. 2. Transfer function of the system relating electrical component of the torque (ΔT_e) produced by voltage regulator action in response to $\Delta\omega$.

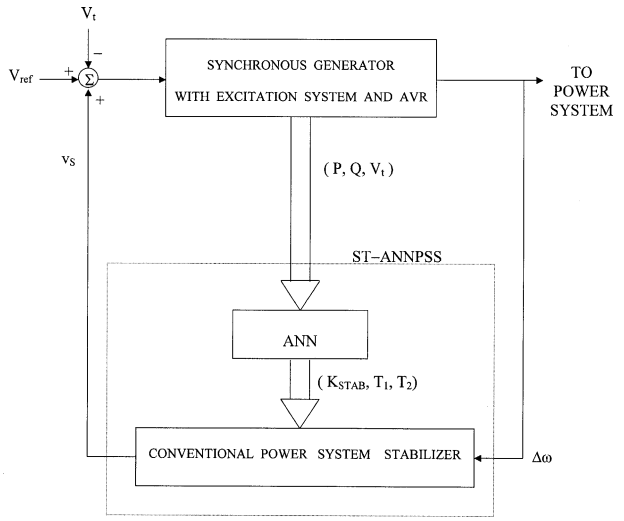

Fig. 3. Schematic diagram of a synchronous generator with self-tuning artificial neural network based power system stabilizer (ST-ANNPSS).

bus voltage E_B are related as

$$\boldsymbol{E_B} = \boldsymbol{V_t} + jX_e\left(\frac{P - jQ}{\boldsymbol{V_t}^*}\right) \tag{2}$$

Let us consider E_B as a reference phasor, and $\boldsymbol{V_t} = V_{td} + jV_{tq}$From Eq. (2), we get

$$E_B = V_{td} - \frac{X_e\left(P\sqrt{V_t^2 - V_{td}^2} - QV_{td}\right)}{V_t^2} \tag{3}$$

$$0 = \sqrt{V_t^2 - V_{td}^2} + \frac{X_e\left(PV_{td} + \sqrt{V_t^2 - V_{td}^2}Q\right)}{V_t^2} \tag{4}$$

The Eqs. (3) and (4) are independent equations in terms of E_B, V_t, P, Q, V_{td} and X_e. Assuming $E_B = 1.0$ p.u., we are left with five variables and two equations. If three of these five variables are assumed then other two can be determined. Thus, the operating condition is characterized by three variables out of the five. Since P, Q and V_t are measurable at the terminals of the generator, these are chosen as the coordinates of the input space. Thus the nodes in the input layer of ANN receive generator real power out put (P), generator reactive power output (Q), and generator terminal voltage (V_t). In the present investigations, two identical lead-lag networks are chosen for the conventional PSS (i.e. $T_1 = T_3$ and $T_2 = T_4$), hence the parameters of the PSS to be tuned in real-time are K_{STAB}, T_1 and T_2. Thus the nodes in the output layer provide the desired PSS parameters K_{STAB}, T_1 and T_2.

4.1. Optimization of parameters of PSS

The phase compensation technique [7] is used for optimizing PSS parameters. It comprises the following steps.

1. Computation of the time constants of the lead networks: The phase angle of the transfer function GEP(s) is computed for $s = j\omega_n$. This phase angle is denoted as γ. The time constants of the lead networks are computed so as to compensate the phase angle of the system. Hence T_1 and T_2 are computed as follows.

$$T_1 = aT_2, \qquad a = (1 + \sin\gamma/2)/(1 - \sin\gamma/2),$$
$$T_2 = 1/(\omega_n\sqrt{a}) \tag{5}$$

2. Computation of stabilizer gain for the desired damping ratio ζ, for the electromechanical mode. The stabilizer gain (K_{STAB}) is computed using the following equation.

$$K_{STAB} = \frac{2\zeta\omega_n M}{K_2|G_c(j\omega_n)||\mathrm{GEP}(j\omega_n)|} \tag{6}$$

Where ω_n = natural frequency of oscillation of the mechanical loop $= \sqrt{(K_1\omega_o/M)}$, $G_c(s)$ = transfer function of the phase compensator $= [(1 + aT_2s)/(1 + T_2s)]^2$, and ζ is desired damping ratio ($\zeta = 0.5$ is assumed in the research work presented here).

4.2. Generation of training patterns

The training set should be so generated that it covers the complete domain of operation [10]. For generating training patterns; P, V_t and X_e are assumed to vary over the typical ranges given as: P: 0.5–1.0 p.u.; V_t: 0.9–1.1 p.u.; X_e: 0.4–0.8 p.u.

A set of 500 operating points is generated, randomly. For each value of P, V_t and X_e, the value of Q is computed. It is important to highlight that P, Q and V_t are chosen as the elements of input vector since these can be measured easily. The input vector now accounts for the variation of X_e. For each of the 500 training points, the optimum parameters of the PSS (K^*_{STAB}, T^*_1 and T^*_2) are computed using phase compensation technique. The output vector of the training patterns, thus, becomes K^*_{STAB}, T^*_1 and T^*_2. The ANN based stabilizers proposed in the past do not account for the variation of equivalent reactance, X_e. With the proposed structure of the ANN, the resulting ST-ANNPSS becomes highly robust.

4.3. Selection of number of neurons in the hidden layer

The architecture of the feedforward ANN comprises an input layer, one or more hidden layers and an output layer.

Table 1
Effect of variation of number of training patterns on SSE (Training) and SSE (Test)

Number of training patterns	SSE (Training)	SSE (Test)
50	0.0172	0.2962
100	0.0443	0.2108
150	0.1264	0.1527
200	0.1362	0.1247
300	0.1427	0.0812
400	0.1990	0.0579
500	0.2569	0.0653

Table 2
Effect of variation of number of neurons in the hidden layer on SSE (Training), SSE (Test), training time and critical clearing time (CCT)

Number of neurons in the hidden layer	SSE (Training)	SSE (Test)	Training time (s)	CCT (s)
4	0.356536	0.212405	191	0.001
5	0.280571	0.248970	249	0.064
6	0.198803	0.057910	295	0.079
7	0.180356	0.057990	396	0.084
8	0.170975	0.067180	501	0.089
9	0.159074	0.06212	552	0.094
10	0.171826	0.06450	714	0.094

For the present investigations, the elements of input vector are P, Q and V_t and that of the output vector are K^*_{STAB}, T^*_1 and T^*_2 hence three neurons are needed in each of the input and the output layers. One hidden layer is chosen to start with. The ANN is trained presenting the training patterns using TRAINLM function of NEURAL NETWORK TOOLBOX of the MATLAB software. In order to arrive at an optimum number of neurons in the hidden layer, following systematic procedure is followed.

The effect of variation of number of neurons in the hidden layer, on the performance of the ST-ANNPSS, is evaluated. The following quantitative indices are considered for evaluating the performance of the ST-ANNPSS.

(a) The sum of squares of errors (SSE) attained at the end of the ANN training. It will be denoted by SSE (Training).
(b) SSE obtained by presenting typical 20 test patterns (not included in the training set) to the trained ANN. The value of SSE so computed will be denoted by SSE (Test).
(c) The critical clearing time (CCT) for a three-phase short circuit at the terminals of the generator cleared by itself (i.e. post-fault system is same as the pre-fault system). Such a fault is called transitory fault. The CCT is obtained for the nominal operating condition and system parameters. The nonlinear mathematical model of the system (Appendix) is used for simulation studies.

Before attempting a study for selection of the adequate number of neurons in the hidden layer, it is important to arrive at the required number of training patterns for training the ANN. The studies are carried out considering six neurons in the hidden layer. The ANN is allowed to continue to train till the reduction in SSE (Training) becomes insignificant.

Table 1 shows the effect of variation of number of training patterns on SSE (Training) and SSE (Test). It may be clearly seen from Table 1 that the SSE (Test) decreases as the number of training patterns is increased from 50 to 400. The SSE (TEST) however, increases as the number of training patterns is increased beyond 400. The gradual increase in SSE (Training) with increase in number of training patterns is due to summation being carried out on larger number of training patterns. The quality of training is judged from the value of SSE (Test). The investigations clearly show that for the present study, a set of 400 training patterns is adequate for training the ANN and hence, 400 training patterns are used for further studies.

Table 2 shows the variation of SSE (Training), SSE (Test), training time and the CCT computed for a transitory three-phase short circuit at the terminals of the generator considering nominal loading and system parameters with the variation of number of neurons in the hidden layer (computations were done using Pentium-100 MHz PC).

It is clearly seen that both SSE (Training) and SSE (Test) decrease while the CCT increases with the increase in number of neurons in the hidden layer from 4 to 9. It is interesting to highlight the fact that with nine neurons in the hidden layer; both SSE (Training) and SSE (Test) attain a minimum value, while CCT becomes constant for number of neurons ≥ 9 in the hidden layer. It may be noted that the training time increases with increase in number of neurons in the hidden layer.

Table 3 shows the optimum PSS parameters (K_{STAB}, T_1 and T_2) computed using trained ANN with nine neurons in

Table 3
PSS parameters computed using trained ANN with nine neurons in the hidden layer and corresponding off-line computed optimum values for 10 test operating conditions

Operating Condition Input vectors				PSS parameters computed using ANN			Optimum PSS parameters computed through off-line studies		
P (p.u.)	Q (p.u.)	V_t (p.u.)	X_e (p.u.)	K_{STAB}	T_1	T_2	K^*_{STAB}	T^*_1	T^*_2
0.73	0.07	0.94	0.56	21.56	0.334	0.064	21.52	0.334	0.064
0.97	0.27	0.99	0.55	22.58	0.330	0.064	22.59	0.329	0.064
0.76	0.19	0.95	0.76	22.31	0.348	0.086	22.15	0.347	0.086
0.99	0.23	0.93	0.58	17.53	0.358	0.076	17.98	0.359	0.076
0.85	0.15	0.96	0.56	21.56	0.335	0.065	21.45	0.335	0.065
0.87	0.07	0.91	0.52	17.98	0.351	0.064	18.22	0.353	0.064
0.60	0.22	1.06	0.51	35.81	0.304	0.063	35.74	0.300	0.057
0.86	0.28	0.98	0.71	22.88	0.340	0.081	22.80	0.341	0.081
0.86	0.28	1.02	0.65	25.46	0.325	0.071	25.35	0.326	0.071
0.90	0.19	0.90	0.65	17.34	0.366	0.086	17.35	0.371	0.087

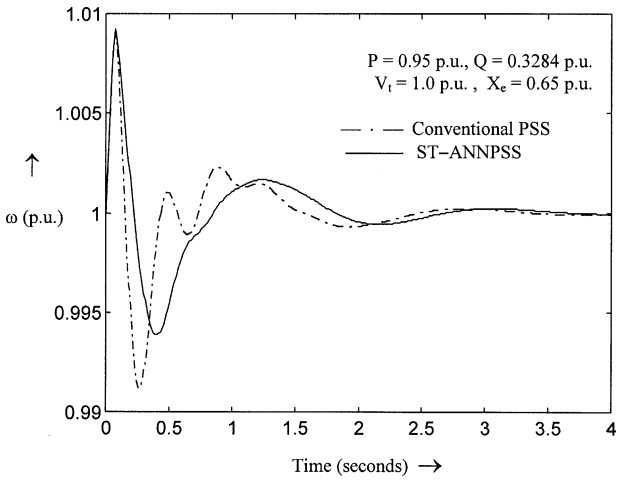

Fig. 4. Dynamic responses for ω considering a transitory 3-phase short circuit of 4 cycles duration at the terminals of the generator, with: (a) ST-ANNPSS, and (b) conventional PSS ($K^*_{STAB} = 22.8418$, $T^*_1 = 0.3360$ sec. and $T^*_2 = 0.0748$ sec.

the hidden layer, and those obtained by off-line computations, for 10 typical test operating conditions (not included in the training set). It is clearly seen that the PSS parameters computed using ANN match very closely with the corresponding off-line computed optimum values.

Studies were also carried out, by adding second hidden layer, and the investigations revealed that there is no merit in adding second layer. Hence, ANN with nine neurons in the hidden layer is chosen for further studies.

4.4. Dynamic performance of the system with ST-ANNPSS

Fig. 3 shows the schematic block diagram used for simulating the dynamic performance of the system with ST-ANNPSS. A sampling period of 10 ms is assumed. The sampled values of P, Q and V_t of the synchronous generator are applied to ANN. The ANN computes the optimum

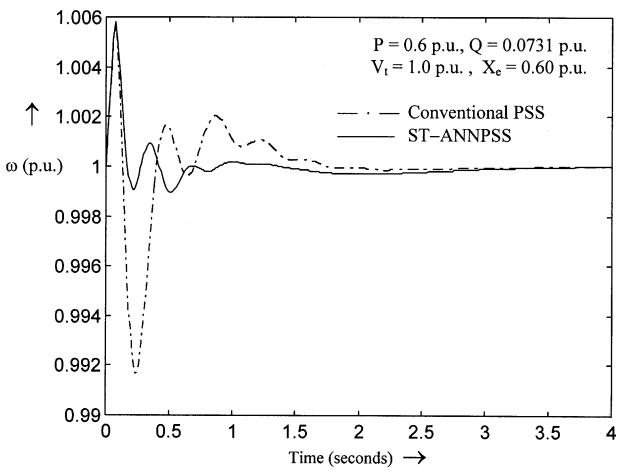

Fig. 5. Dynamic responses for ω considering a transitory 3-phase short circuit of 4 cycles duration at the terminals of the generator, with: (c) ST-ANNPSS, and (d) conventional PSS ($K^*_{STAB} = 22.8418$, $T^*_1 = 0.3360$ sec. and $T^*_2 = 0.0748$ sec.

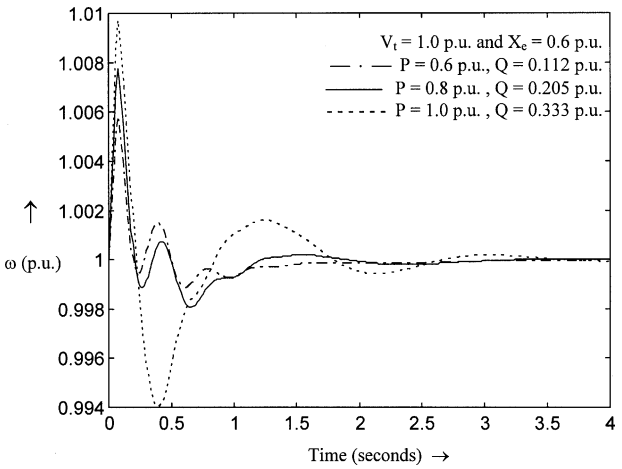

Fig. 6. Dynamic responses for ω considering a transitory 3-phase short circuit of 4 cycles duration at the terminals of the generator.

values of PSS parameters (K^*_{STAB}, T^*_1 and T^*_2). The stabilizing signal, v_S is computed by the PSS using the K^*_{STAB}, T^*_1, T^*_2 and $\Delta\omega$. During the sampling period, the stabilizing signal so computed remains constant. Dynamic responses of the system are obtained considering a transitory three-phase short circuit of four cycles duration at the terminals of the generator.

The dynamic responses of the system at nominal operating condition for ω (Fig. 4) are obtained with: (a) ST-ANNPSS and (b) conventional PSS.

Examination of Fig. 4 clearly reveals that the dynamic response obtained with ST-ANNPSS is virtually identical to that obtained with optimum conventional PSS ($K^*_{STAB} = 22.8418$, $T^*_1 = 0.3360$ s and $T^*_2 = 0.0748$ s).

Further, the dynamic response for ω (Fig. 5) is obtained for an operating condition of the system quite different from the nominal i.e. $P = 0.6$ p.u., $Q = 0.0731$ p.u., $V_t = 1.0$ p.u. and $X_e = 0.4$ p.u, with (a) ST-ANNPSS and (b) conventional PSS (Tuned for the nominal operating condition i.e. $K_{STAB} = 22.8418$, $T_1 = 0.3360$ s and $T_2 = 0.0748$ s). It is clearly seen

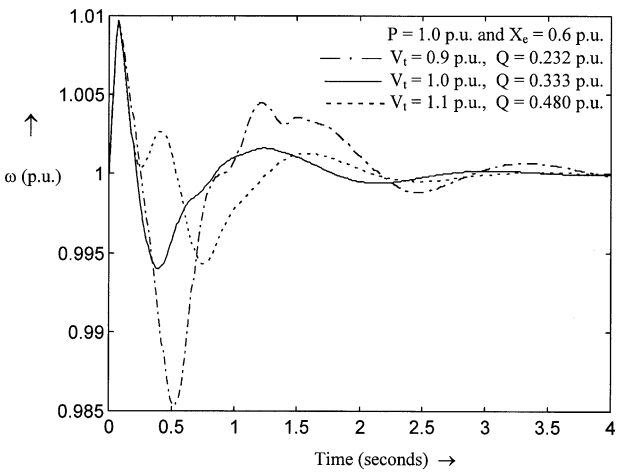

Fig. 7. Dynamic responses for ω considering a transitory 3-phase short circuit of 4 cycles duration at the terminals of the generator.

that while the dynamic response with conventional PSS is significantly affected, the dynamic performance with ST-ANNPSS remains well damped even with substantial shift in operating condition from the nominal.

4.5. Effect of variation of loading condition

The dynamic performance of the system with ST-ANNPSS is now evaluated over a wide variation in loading condition. Following five typical loading conditions spread over the entire domain of operation for which the ANN was trained, are chosen for assessing the robustness of the ST-ANNPSS:

1. $P = 0.6$ p.u., $Q = 0.112$ p.u. and $V_t = 1.0$ p.u.
2. $P = 0.8$ p.u., $Q = 0.205$ p.u. and $V_t = 1.0$ p.u.
3. $P = 1.0$ p.u., $Q = 0.333$ p.u. and $V_t = 1.0$ p.u.
4. $P = 1.0$ p.u., $Q = 0.232$ p.u. and $V_t = 0.9$ p.u.
5. $P = 1.0$ p.u., $Q = 0.480$ p.u. and $V_t = 1.1$ p.u.

It may be noted that the equivalent reactance, $X_e = 0.60$ p.u. is considered for all the above operating conditions. The dynamic responses for ω are obtained considering a transitory three-phase short circuit of four cycles duration at the terminals of the generator. Examining the responses (Figs. 6 and 7), it may be concluded that the system dynamic performance with ST-ANNPSS is quite robust over the entire domain of loading.

5. Conclusions

A systematic approach for designing a ST-ANNPSS has been presented. A new approach for the selection of number of neurons in the hidden layer of the ANN has been proposed. Investigations show that ANN with one hidden layer comprising nine neurons is adequate and sufficient for ST-ANNPSS. Studies show that the dynamic performance with ST-ANNPSS is virtually identical to that obtained with conventional PSS at the nominal operating condition. However, the dynamic performance of ST-ANNPSS is quite superior to that of conventional PSS for the loading condition different from the nominal. Investigations also reveal that the performance of ST-ANNPSS is quite robust to a wide variation in loading condition.

Acknowledgements

The authors gratefully acknowledge the financial support received from Department of Science and Technology, Power Grid Corporation India Limited ABB, and AICTE (R & D/2001–02/8020-91), which made it possible to conduct this research. The first author gratefully acknowledges the support and encouragement received from the management of GE Power Services (I) Limited.

Appendix

The nominal parameters of the system are given below. All data are in per unit, except M and the time constants. M and the time constants are expressed in seconds [9].

$M = 2H = 7.0$, $P = 0.95$, $V_t = 1.0$, $E_B = 1.0$, $X_d = 1.81$, $X_q = 1.76$, $X'_d = 0.3$, $L_{adu} = 1.65$, $X_l = 0.16$, $R_a = 0.003$, $R_{fd} = 0.0006$, $L_{fd} = 0.153$, $K_A = 50$, $T_R = 0.02$, $T_A = 0.05$, $X_e = 0.65$, $R_e = 0.0$,

The system frequency $f_o = 60$ Hz..

The nonlinear dynamic model of the system is given below:

$$\dot{\omega} = (T_m - T_e)/2H$$

$$\dot{\delta} = \omega_o(\omega - 1)$$

$$\dot{E}'_q = [E_{fd} - (E'_q + (X_d - X'_d)I_d)]/T'_{do}$$

$$\dot{E}_{fd} = [K_A(V_{ref} - V_t) + v_S) - E_{fd}]/T_a$$

where

$$T_e = V_{td}I_d + V_{tq}I_q$$

$$V_t = \sqrt{(V_{td}^2 + V_{tq}^2)}$$

$$V_{td} = X_qI_q$$

$$V_{tq} = E'_q - X'_dI_d$$

$$I_d = [(X_e + X_q)(E'_q - E_B \cos\delta) - E_BR_e \sin\delta]/Z_e^2$$

$$I_q = [R_e(E'_q - E_B \cos\delta) + (X_e + X'_d)E_B \sin\delta]/Z_e^2$$

$$E'_q = V_{tq} + X'_dI_d$$

$$Z_e^2 = R_e^2 + X_e^2 + X_e(X_q + X'_d) + X_qX'_d$$

$$E_B = \sqrt{[(V_{to} - I_dR_e + I_qX_e)^2 + (I_qR_e + I_dX_e)^2]}$$

For the nominal loading condition $E_{fd} = 2.506$ p.u. and $i_{fd} = 1.5161$ p.u.

References

[1] Hsu Y-Y, Chen C-R. Tuning of power system stabilizers using an artificial neural network. IEEE Trans Energy Conversion 1991;6(4):612–9.
[2] Zhang Y, Chen GP, Malik OP, Hope GS. An artificial neural network based adaptive power system stabilizer. IEEE Trans Energy Conversion 1993;8(1):71–7.
[3] Zhang Y, Malik OP, Chen GP. Artificial neural network power system stabilizers in multi-machine power system environment. IEEE Trans Energy Conversion 1995;10(1):147–54.
[4] Guan L, Cheng S, Zhou R. Artificial neural network power system stabilizer trained with an improved BP algorithm. IEE

Proceedings on Generation Transmission Distribution 1996; 143(2):135–141.

[5] Park YM, Lee KY. A neural network based power system stabilizer using power flow characteristics. IEEE Trans Energy Conversion 1996;11(2):435–41.

[6] De Mello FP, Concordia C. Concepts of synchronous machine stability as affected by excitation control. IEEE Trans Power Apparatus Syst 1969;PAS-88(4):316–29.

[7] Yu Y-N. Electric power system dynamics. London: Academic Press; 1983.

[8] Anderson PM, Fouad AA, Fouad, power system control and stability, vol. 1. AMES, IOWA: The Iowa State University Press; 1977.

[9] Kundur P. Power system stability and control. New York: McGraw Hill; 1994.

[10] Haykin S. Neural networks—a comprehensive foundation. NewYork: Macmillan College Publishing Company; 1994.